

Creative Commons Attribution 4.0 International (CC BY 4.0)

<https://creativecommons.org/licenses/by/4.0/>

Access to this work was provided by the University of Maryland, Baltimore County (UMBC) ScholarWorks@UMBC digital repository on the Maryland Shared Open Access (MD-SOAR) platform.

**Please provide feedback**

Please support the ScholarWorks@UMBC repository by emailing [scholarworks-group@umbc.edu](mailto:scholarworks-group@umbc.edu) and telling us what having access to this work means to you and why it's important to you. Thank you.

## Article

# AIRS satellite CO data confirm the increase in wildfires in the Northern Hemisphere over the past two decades.

Leonid Yurganov <sup>1\*</sup><sup>1</sup> University of Maryland Baltimore County, Baltimore, MD, 21250, USA (retired)

\* Correspondence: leonid.yurganov@gmail.com;

**Abstract:** Biomass burning is an important and changing component of the global and hemispheric carbon cycles. In particular, boreal forest fires in Russia and Canada are important sources of greenhouse gases carbon dioxide (CO<sub>2</sub>) and methane (CH<sub>4</sub>). The influence of carbon monoxide (CO) on the climate is insignificant: its main absorption bands of 4.6 and 2.3  $\mu\text{m}$  are far away from the climatically important regions of the spectrum. Meanwhile, CO concentrations in fire plumes are closely related to CO<sub>2</sub> and CH<sub>4</sub> emissions from fires. On the other hand, satellite measurements of CO are much simpler than those for the aforementioned gases. The Atmospheric Infrared Sounder (AIRS) provides a long satellite-based CO data set. This article presents estimates of CO emissions from biomass burning north of 30° N using a simple two-box model. These results correlate closely with independently estimated CO emissions from the GFED4 bottom-up data base. Both ones reported record high emissions in 2021 throughout two decades, double the annual emissions comparing to the previous a few years. There have been several years with extreme emissions, but for the rest of data upward trend with a rate of  $3.7 \pm 2.3 \text{ Tg CO yr}^{-2}$  ( $4.4 \pm 2.8\%$  per year), was found.

**Keywords:** Thermal Infrared satellite data; carbon monoxide; boreal fires; carbon dioxide

## 1. Introduction

Boreal forest fires (wildfires) in the Northern hemisphere have various impacts on the environment and on the climate system. Changes in evapotranspiration, surface heat regime, productivity and soil respiration, postfire changes of albedo on the burned areas and many other effects are just some examples of adverse climatic effects [1]. Emissions of greenhouse gases are in the row of these phenomena. Estimating the amount of greenhouse gases emitted by natural fires is not simple. A so called "bottom-up" approach assimilates data on dry organic matter per unit of burned area, emission factors for specific gases, and types of burning and/or smoldering [2]. Many parameters in these calculations are not known accurately. Especially, Siberian fires are most difficult objects due to extremely rare ground network of observations. Nevertheless, a significant progress has been achieved by now in this technique [3].

In another approach, called "top-down" or "inversion", the magnitude of GHG emissions are retrieved from measurements of gas concentrations in the atmosphere from different sensors, ground-, aircraft-, or satellite-based. The advantage of satellite concentration measurements over others is their global coverage. The main disadvantage of satellite methods is their low accuracy for the planetary boundary layer that is primarily polluted by fires. Therefore, they need to be corrected for lower sensitivity by comparison with more accurate ground based spectroscopic measurements. As a matter of fact, the combination of these two independent approaches for the study of greenhouse gas emissions appears to be the most reliable.

Two longest satellite CO data sets are available. The Measurement Of Pollution in The Troposphere (MOPITT, 2000 - now) [4] and Atmospheric Infrared Sounder (AIRS,

2002 - now) [5] supply global total columns (TC) and profiles. According to MOPITT, carbon monoxide annual concentrations have declined since 2000. The decrease is particularly noticeable in the Northern Hemisphere. Most of air quality experts attribute this decline to technological and regulatory innovations in transport and industry [4]. Summertime year-to-year CO fluctuation were caused by biomass burning changes [6].

The first attempt to estimate CO emissions from 2002-2003 fires from MOPITT data combined with ground-based samplings in the High Northern hemisphere (HNN, 30° N - 90° N) was undertaken based on a mass-balance model [6]. This model was developed before that for studying 1998 boreal fires [7]. An alternative to a box model is a global three-dimensional transport model. Such model [8] has been applied to the MOPITT data set for 2000-2019 [9], and inferred surface total fluxes of CO at a spatial resolution of 3.75° longitude × 1.9° latitude.

In this paper we estimated the HNN fire CO emissions from 2002 to 2021 using a box model described in previous publications [6, 7] with the same parameters (e.g., photochemical removal, air exchange between tropical and extratropical Northern hemisphere, etc). A comparison with independent GFED4 estimates [3] demonstrated a reasonable random differences between two data sets less than  $\pm 10 \text{ Pg CO mon}^{-1}$  for most of the data with exception of just a few points. Both GFED4 bottom-up and AIRS top-down techniques clearly reveal increasing trend in wildfire emissions over last 20 years.

## 2. Materials and Methods

### 2.1. AIRS data and validation

AIRS is a diffraction grating spectrometer that was launched in a sun-synchronous polar orbit in May 2002 on board the Aqua satellite [5]. The instrument scans  $\pm 48.3^\circ$  from the nadir, which provides almost full global daily coverage. Spectral resolution is  $1.79 \text{ cm}^{-1}$  at the CO fundamental absorption band near  $4.6 \mu\text{m}$  wavelength. Currently (June, 2022), the AIRS is still operational. A new version 7 of the data [10] is characterized by: improved consistency between day and night water vapor, improved temperature products, improved AIRS IR only retrievals, especially in the high latitude regions, removal of ambiguity in surface classification in the infrared-only (IR-only) retrieval algorithm. Monthly and daily average Level 3 between October, 2002 and April, 2022, both ascending and descending orbits, are available on-line on a  $1^\circ \times 1^\circ$  latitude/longitude grid: <https://disc.gsfc.nasa.gov/datasets/>, AIRS3STM 7.0 (monthly) and AIRS3STD 7.0. (daily). A reduced sensitivity of AIRS required a correction coefficient (see section 3.1).

The chosen box model deals with monthly total amounts of gas in the box. For our needs we average the total column CO for ascending orbits in  $\text{molec cm}^{-2}$  (or the vertically averaged volume mixing ratio  $X_{\text{CO}}$  in ppb) and multiply that by the area of the box in molecules or in Tg CO.  $X_{\text{CO}}$  for validation are regularly recorded by Bruker IFS 125HR sun-tracking Fourier Transform interferometers at the Total Carbon Column Observing Network (TCCON) [11]. The AIRS L3 daily means for the grid cells coinciding with nine locations of validation sites (Table 1) were compared with  $X_{\text{CO}}$  determined from the ground.

### 2.2. Mass-balance box model

A box model approach is an alternative to a global chemical transport model (CTM). It is based on a general idea of a relatively slow exchange of air between the HNN and the Low Northern hemisphere (LNH, between the equator and 30° N). Wildfires emit CO and this excess CO is quickly spread over the HNN. Leaks to the LNH (transport loss) were estimated from an available CTM model [7, 12]. A significant part of the pyrogenic CO is quickly oxidized by tropospheric hydroxyl OH and should be carefully counted as well.

A calculation procedure was as follows:

1. Satellite-measured CO volume mixing ratio profiles was averaged over each box and converted into molec cm<sup>-2</sup>.
2. The average seasonal cycle over 48 months after January 2004 was calculated.
3. The CO trend was calculated for February-March months of all years using fifth order polynomial approximation and applied to all data.
5. The HNH-averaged CO TC was subtracted by the trend and the seasonal cycle to represent the anomaly. Then it was multiplied by the area of the box, and converted in Tg (M'<sub>HNH</sub>).
6. The anomaly was divided by 0.7 (see validation below) to correct for a reduced sensitivity.
7. Loss terms in the Eqs. 2 and 3 were calculated.
8. The wildfire emission P' was calculated as a sum of monthly changes of M'<sub>HNH</sub> and two loss terms, transport into the LNH, L<sub>trans</sub>, and loss of CO due to a reaction with hydroxyl (OH), L<sub>chem</sub>; quote marks mean deviations from the 2004-2007 background.

$$P' = M'_{\text{HNH}}/dt + L_{\text{trans}} + L_{\text{chem}}, \quad (1)$$

$$L_{\text{trans}} = (M_{\text{HNH}} - M_{\text{LNH}})/\tau_{\text{trans}}, \quad (2)$$

$$L_{\text{chem}} = M'_{\text{HNH}}/\tau_{\text{chem}}, \quad (3)$$



$$\tau_{\text{chem}} = 1/[\text{OH}] \cdot k, \quad (5)$$

$$k = 1.5 \cdot 10^{-13} (1 + 0.6 \cdot P) \text{ cm}^3 \text{ molec}^{-1} \text{ s}^{-1}, \quad (6)$$

where  $\tau_{\text{trans}}$  was calculated using a 3-D GEOS-CHEM global CTM [12] and found as 2.5 months on average ([7]. [OH] is the hydroxyl concentration [13] averaged over HNH, k is the reaction (4) rate constant [14], P is air pressure in hPa.  $\tau_{\text{chem}}$  varied between 1.4 and 27 months in July and in December, respectively [7].

### 3.1. Validation results

The ground-based TCCON CO measurements for July-August were used for validation. Figure 1 summarizes comparisons between daily mean  $X_{\text{CO}}$  measured by FTIRs ("ground truth") and the AIRS. Parameters of the least squares linear regression are listed in Table 1. All stations are located to the north of 30° N. Averaged slope of regression lines is  $0.70 \pm 0.12$  ppb/ppb. Physical meaning of the slope is the empirical sensitivity: a response of AIRS-derived  $X_{\text{CO}}$  to a unity change of the true value. Average slope was used for correction of AIRS-detected CO variations. Complicated relief patterns and/or urban influence for some sites (e.g., Caltech, Pasadena) caused a bias between the two data sets.

3. Results of CO measurements and emission estimates

3.1. Xco measured by AIRS

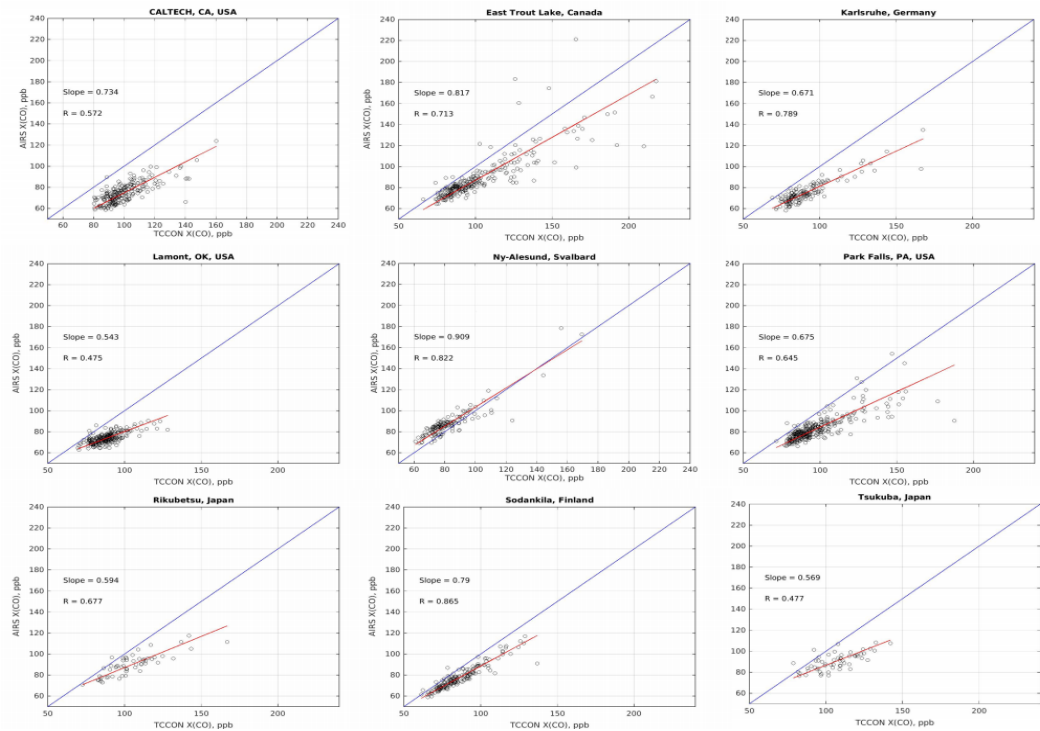


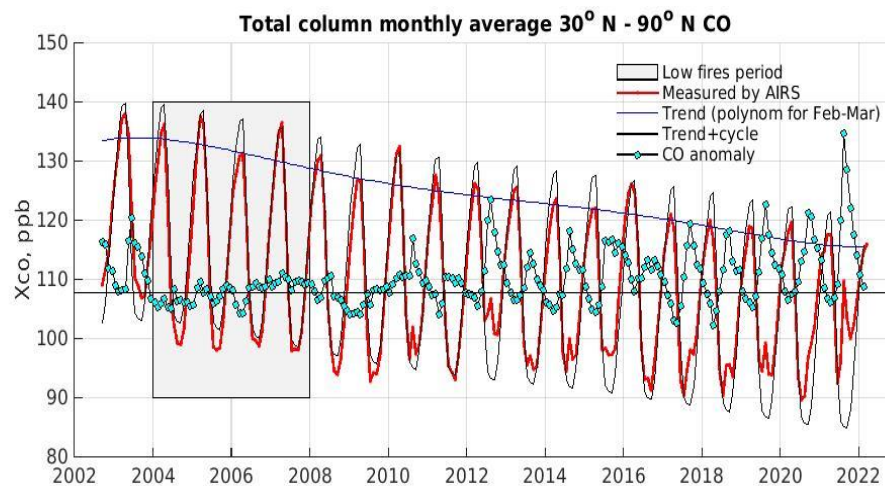
Figure 1. Daily mean Xco measured by AIRS and by ground-based FTIRs on the TCCON network.

Table 1. TCCON validation sites. Locations and parameters of linear regression.

Site	Latit.; Longit.	Slope	Interseption	R
Caltech, CA, USA	34.136 ; -118.127	0.73	1.52	0.571
E. Trout Lake, Canada	54.35 ; -104.99	0.816	5.42	0.712
Karlsruhe, Germany	49.1; 8.438	0.670	14.21	0.788
Lamont, OK, USA	36.604; -97.486	0.542	26.11	0.474
Ny-Alesund, Svalbard	78.9 ; 11.9	0.908	12.72	0.822
Park Falls, PA, USA	45.945; -90.273	0.675	16.99	0.644
Rikubetsu, Japan	43.4567; 143.7661	0.593	27.67	0.677
Sodankyla, Finland	67.3668; 26.631	0.790	9.67	0.864
Tsukuba, Japan	36.0513 ; 140.1215	0.568	29.80	0.477

Figure 2 presents original AIRS measurements and trends. CO column amounts are impacted by emissions from incomplete combustion in transport and industry. Improvements in technology that diminishes anthropogenic emissions result in a long-term downward trend. Seasonal variations with a maximum in March and minimum in August [15] are governed mostly by changes of OH concentrations. Maximum effect of biomass burning is observed in summer. Both inter-annual changes and increasing trend of summer CO are obvious on the original record. A period of minimal summer variations (2004-2007) was taken for calculation of the unperturbed seasonal cycle. The original data were modified in attempt to exclude the trend and the seasonal changes. The trend was determined from late winter February-March data and applied to the whole results. Therefore, the thin black line represents a "background". In other words, this line represents Xco in absence of biomass burning emissions. A difference between red line (measured Xco) and thin black line (background) was attributed to the net effect of biomass burning (green dots). Most striking is a breaking-record CO spike in August

2021. Note a fast increase between June and August in each year caused by fires and a decay afterwards due to photochemical and transport removals. Validation, described above, revealed a ~30% underestimation for any AIRS-measured change of Xco. The change in Xco caused by fires was consequently corrected and after that was used as input for the box model.



**Figure 2.** Original data, trend, seasonal cycle, and fire-driven anomaly of Xco. Units are vertically averaged mixing ratio in ppb.

### 3.2. Fire emissions

Monthly HNH CO fire emissions calculated using our box model are plotted in Figure 3 as a function of time. As a rule, maximal emissions occurred in July, sometime in August. The months of maximal concentration (e.g., August in 2021) normally followed the months of maximum emission (July in 2021). GFED4 CO data are in agreement with AIRS data. A scatter plot (Figure 4) evidences a close correlation between monthly emissions obtained by these two independent methods (slope is  $0.81 \pm 0.5$ , correlation coefficient  $R = 0.69$ ). Absolute values of emissions differ less than 10 Tg/month for most of data, only three encircled summer points scattered out. In all 3 cases AIRS data were lower than emissions assessed by GFED4. These months (July and August) coincide with most strong fires. It is reasonable to assume that this extra CO locates in lowest layers of the troposphere, where the sensitivity of TIR instruments drops down. To validate remote sensing with more representativeness one need ground truth sites that are closer to the fire areas then the TCCON sites are (see above).



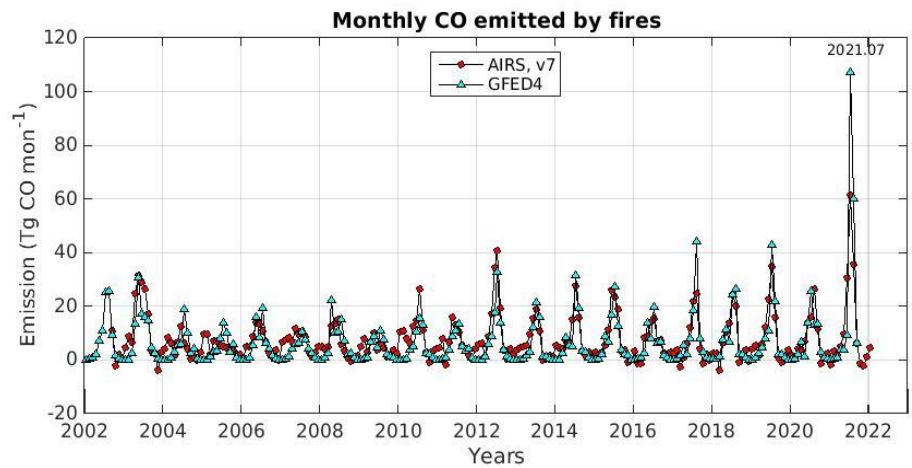


**Figure 3.** Monthly CO emissions from fires estimated from AIRS data and compared with GFED4 results [3].

Annual emissions of CO from AIRS and GFED4 are presented in Figure 5 and Table 2. Corresponding CO<sub>2</sub> emissions (for GFED4 only) are plotted in Figure 5 for comparison. After two years of strong fires in 2002 and 2003 [6] a relatively gradual increase in annual emissions was observed. Regression lines over 2004-2020 for AIRS (red) and for GFED4 (blue) are parallel: slopes are  $3.7 \pm 2.3$  and  $3.5 \pm 1.3$  Tg CO year<sup>-2</sup>, respectively. 95% confidence intervals were obtained as described by [16]. CO<sub>2</sub> fire emission increases with the rate  $43.6 \pm 17$  Tg CO<sub>2</sub> yr<sup>-2</sup>. The fires of 2021 set a new record.

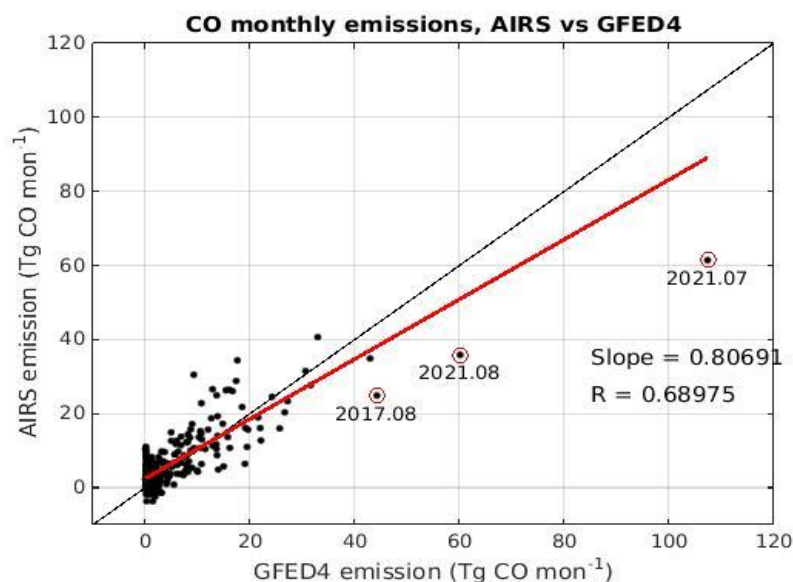


**Figure 4.** Monthly CO emitted by fires in HNH according to AIRS in comparison with GFED4 data [3]. Times for most scattered points are labeled.

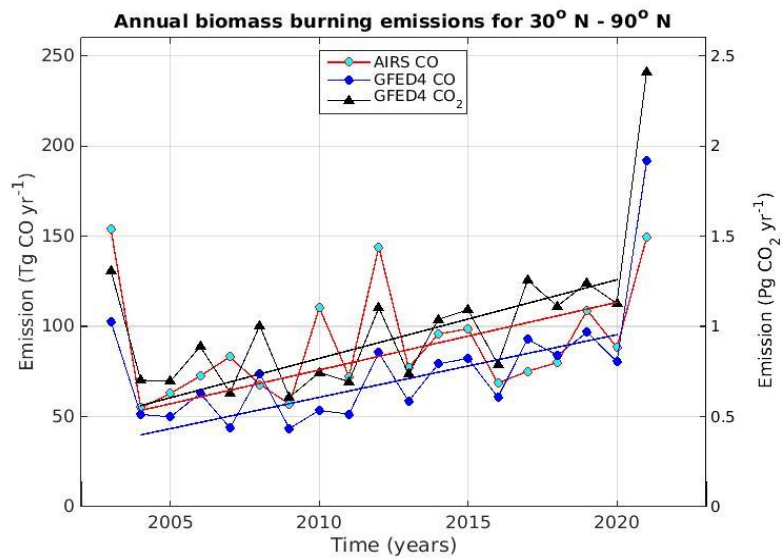


**Figure 5.** Annual CO emitted by fires in HNH according to AIRS data and a bottom-up GFED4 estimates [3]. CO<sub>2</sub> emission (right scale) is plotted for comparison [3]. Least squares regression lines are shown as well.

**Table 2.** Annual HNH CO fire emissions in Tg yr<sup>-1</sup> for this paper and from [6]

Year	AIRS (this paper)	GFED4 (this paper)	FTIR [6]	MOPITT [6]
1998		114	151.4	
1999		48	32.3	
2000		50	-1.8	1.8
2001		43	5.1	-0.9
2002		83	120.6	73.5
2003	154	103	160.6	118.0
2004	55	51		
2005	63	50		
2006	72	63		
2007	83	44		
2008	68	74		
2009	57	43		
2010	110	53		
2011	72	51		
2012	144	85		
2013	77	58		
2014	96	79		
2015	99	82		
2016	68	61		
2017	75	93		
2018	80	84		
2019	109	97		
2020	88	80		
2021	149	195		



#### 4. Discussion

Remote sensing satellite measurements combined with a box model allows a fast, actually immediate, monitoring of forest fires CO emission on a hemispheric or global scale. A comparison with bottom-up approaches (like GFED) raises validity of conclusions.

Our satellite results (Table 2) revealed 2004-2020 mean HNH CO emission as  $83 \pm 23 \text{ Tg CO yr}^{-1}$  with a quasi-linearly growing trend  $3.7 \pm 2.3 \text{ Tg CO year}^{-2}$  ( $4.4 \pm 2.8\% \text{ yr}^{-1}$ ). Agreement between top-down and bottom-up GFED4 approaches on a monthly basis is an additional proof for this conclusion. No doubt that 2021 fires set a new record of emission. The inversion of AIRS data for July 2021 (Figures 3 and 4) resulted in just a half of GFED4 estimate. This disagreement does not look as a random fluctuation. We consider this underestimation as a result of unaccounted effect of reduced sensitivity of AIRS to lower altitudes. The validation was based for ground truth sites that were far away from burning areas. So the annual emission of  $195 \text{ Tg CO yr}^{-1}$  should be closer to reality. A possibility of further acceleration can not be excluded, though a detailed investigation of reasons for the fire intensification is beyond the scope of this publication.

Global 2000–2019 CO fire emission inferred from MOPITT data [17] was reported to have insignificant decline of  $-0.7 \pm 1.0\% \text{ yr}^{-1}$ . Mean Northern hemispheric estimates were not presented, but Canada and Alaska were noted as the regions where both burned areas and emission intensities increased rapidly, driving a substantial increase in its fire CO<sub>2</sub> (and probably CO) emissions from the 2000s to the 2010s.

A good correlation between the two independent estimates of CO fire emission adds confidence to all GFED4 results, and in particular, CO<sub>2</sub>. Their estimates may be compared to the anthropogenic production. Global fossil carbon dioxide emissions [18] we estimated as 34.8 and 36.2 Pg CO<sub>2</sub> yr<sup>-1</sup>, for 2020 and 2021, respectively, i.e. **1.4 Pg CO<sub>2</sub>** annual increase. The GFED4 database estimate global and HNH CO<sub>2</sub> biomass burning emission as 6.71 (1.13) and 7.70 (2.46) Pg CO<sub>2</sub> yr<sup>-1</sup> (HNH in brackets) in the same years, i.e. **0.98 and 1.33 Pg CO<sub>2</sub>** annual global and HNH increases, respectively. Therefore, the 2021 boreal fires emissions may compete with global fossil CO<sub>2</sub> discharge at least for yearly increments.

**Funding:** This research received no external funding

**Data Availability Statement:** Publicly available datasets were analyzed in this study. These data can be found here: AIRS, AIRS3STM 7.0, AIRS3STD 7.0, <https://disc.gsfc.nasa.gov/datasets/>. GFED4: <https://www.geo.vu.nl/~gwerf/GFED/GFED4/>. TCCON: <https://data.caltech.edu/records/20140>.

**Acknowledgments:** The author expresses his gratitude to Andrey Lapenis (University of Albany, New York, USA) for helpful discussions, to Guido van der Werf (Vrije Universiteit Amsterdam, the Netherlands) for detail explanation of GFED4 data set, and to Debra Wunch (University of Toronto, Ontario, Canada) for a guidance in using TCCON validation data.

**Conflicts of Interest:** The author declares no conflict of interest.

#### References

- 1 Kasischke, E; Stocks, B. *Fire, climate change, and carbon cycling in the boreal forest*; Springer-Verlag: New York, NY, USA, 2000; 461 p.
- 2 Seiler, W.; Crutzen, P.J. Estimates of gross and net fluxes of carbon between the biosphere and the atmosphere from biomass burning. *Clim. Change* **1980**, *2*, 207–247
- 3 Van der Werf, G. R.; Randerson, J. T.; Giglio, L.; van Leeuwen, T. T.; Chen, Y.; Rogers, B. M.; Mu, M.; van Marle, M. J. E.; Morton, D. C.; et al. Global fire emissions estimates during 1997–2016. **2017** *Earth Syst. Sci. Data* *9*, 697–720 .
- 4 Deeter, M.; Francis, G.; Gille, J.; Mao, D.; Martínez-Alonso, S.; Worden, H.; McKain, K. The MOPITT Version 9 CO product: Sampling enhancements and validation. *Atmosph. Meas. Tech.*, **2022** *15*, 2325–2344. doi:10.5194/amt-15-2325-2022

- 5 Aumann, H. H. ; Chahine, M. T.; Gautier, C.; Goldberg M. D.; Kalnay,E.; McMillin, L. M.; Revercomb, H.P.; Rosenkranz, P.W.; Smith, W. L.; Staelin, D. H. et al. AIRS/AMSU/HSB on the Aqua mission: design, science objectives, data products and processing systems. **2003** *IEEE Trans. Geosci. Rem. Sens.*, 41, 253-264.
- 6 Yurganov, L. N.; Duchatelet, P.; Dzhola, A. V.; Edwards, D. P.;Hase, F.; Kramer, I.; Mahieu, E.; Mellqvist, J.; Notholt, J.; Novelli, P. C.; Rockmann, et al. : Increased Northern Hemi-spheric carbon monoxide burden in the troposphere in 2002 and2003 detected from the ground and from space; **2005** *Atmos. Chem.Phys.*, 5, 563–573, doi:10.5194/acp-5-563-2005,.
- 7 Yurganov, L. N.; Blumenstock, T.; Grechko, E. I.; Hase, F.; Hyer,E. J.; Kasischke, E. S.; Koike, M.; Kondo, Y.; Kramer, I.; Le-ung, F.-Y., :A quantitative assessment of the 1998 carbon monoxide emis-sion anomaly in the northern hemisphere based on total column and surface concentration measurements, **2004** *J. Geophys. Res.*, 109,D15305, doi:10.1029/2004JD004559,.
- 8 Zheng, B.; Chevallier, F.; Yin, Y.; Ciais, P.; Fortems-Cheiney, A.; Deeter, M. N.;R. J. Parker,Y. Wang, H. M. Worden, Zhao, Y. . Global atmospheric carbon monoxide budget 2000-2017 inferred from multi-species atmospheric inversions. **2019** *Earth Syst. Sci. Data*, 11, 1411-1436. doi:10.5194/essd-11-1411-2019
- 9 Zheng, B.,Ciais, P. ; Chevallier A , Chuvieco E ; Chen Y ; Yang H Increasing forest fire emissions despite the decline in global burned area **2021** *Sci. Adv.*; 7 : eabh2646
- 10 Tian B; Manning R J; Thrastarson H; Eric Fetzer, E.; Monarrez, R.. **2020** AIRS Version 7 Level 3product user guide. [https://docserver.gesdisc.eosdis.nasa.gov/public/project/AIRS/V7\\_L3\\_User\\_Guide.pdf](https://docserver.gesdisc.eosdis.nasa.gov/public/project/AIRS/V7_L3_User_Guide.pdf).
- 11 Wunch, D.; Toon, G. C.; Blavier, J.-F. L.; Washenfelder, R. A.; Notholt, J.; Connor, B. J.; Griffith, D. W. T.; Sherlock, V.; and Wennberg, P. O.: The Total Carbon Column Observing Network, **2011** *Philosophical Transactions of the Royal Society A: Mathematical, Physical and Engineering Sciences*, 369, 2087-2112,.
- 12 Holloway, T.; Levy II,H.; Kasibhatla,P. Global distribution of carbon monoxide, *J. Geophys. Res.*, 105, 12,123 – 12,147, 2000.
- 13 Spivakovsky, C. M.; Logan, J. A.; Montzka, S. A.; et al.: Three-dimensional climatological distribution of tropospheric OH: Update and evaluation, **2000** *J. Geophys. Res.*, 105(D7), 8931–8980,.
- 14 DeMore, W. B.; Sander, S. P.; Golden, D. M.; Hampson, R. F.;Kurylo, M. J.; Howard, C. J.; Ravishankara, A. R.; Kolb, C. E.;and Molina, M. J. Chemical kinetics and photochemical data for use in stratospheric modeling, **1997** *JPL Publ.*, 97-4,.
- 15 Dianov-Klokov, V. I. and Yurganov, L. N. A spectroscopic study of the global space-time distribution of atmospheric CO, **1981**, *Tellus* 33, 262–273.
- 16 Chatterjee, S.; Hadi A S Influential observations, high leverage points, and outliers in linear regression **1986** *Stat. Sci.* Vol. 1, pp. 379-416.
- 17 Zheng B; Ciais P.; Chevallier F.; Chuvieco E.; Chen Y.; Yang H. Increasing forest fire emissions despite the decline in global burned area **2021** *Sci Adv* 24;7(39):eabh2646. doi: 10.1126/sciadv.abh2646
- 18 Jackson, R.B.; Friedlingstein, P Le Quéré; C; Abernethy, S.; RM Andrew, R.M.; Canadell, J.C.; Ciais; P., Davis, S.J. Deng, Z; Liu,Z., et al., Global fossil carbon emissions rebound near pre-COVID-19 levels **2022** *Environ. Res. Lett.* 17: 031001 doi <https://iopscience.iop.org/article/10.1088/1748-9326/ac55b6>